A Novel Alternating Phenylenevinylene Copolymer with Perylene Bisimide Units: Synthesis, Photophysical, Electrochemical, and Photovoltaic Properties

ARTICLE *in* THE JOURNAL OF PHYSICAL CHEMISTRY C · APRIL 2009

Impact Factor: 4.77 · DOI: 10.1021/jp901651z

A Novel Alternating Phenylenevinylene Copolymer with Perylene Bisimide Units: Synthesis, Photophysical, Electrochemical, and Photovoltaic Properties

John A. Mikroyannidis,*,† Minas M. Stylianakis,† G. D. Sharma,*,‡ P. Balraju,‡ and M. S. Roy§

Chemical Technology Laboratory, Department of Chemistry, University of Patras, GR-26500 Patras, Greece, Physics Department, Molecular Electronic and Optoelectronic, JNV University, Jodhpur 342005, India, and Defence Laboratory, Jodhpur 342005, India

Received: February 23, 2009; Revised Manuscript Received: March 13, 2009

An alternating phenylenevinylene copolymer **P** bearing perylene bisimide moieties along the backbone was synthesized by Heck coupling. The *tert*-butyl and hexyloxy side groups enhanced the solubility of the copolymer in common organic solvents. It had glass transition and decomposition temperatures of 72 and 370 °C, respectively. The absorption of **P** was broad, with longer wavelength maximum around 500 nm and optical band gap of 1.66 eV. The solution of **P** emitted yellow−orange light with photoluminescence (PL) maximum at 555 nm. Moreover, efficient interaction and charge/energy transfer between the phenylenevinylene−donor and the perylene bisimide−acceptor led to PL quenching in the thin film of **P**. The current−voltage characteristics of ITO/copolymer **P**/Al indicated that copolymer **P** behaved as an n type organic semiconductor. The electron current was found to be a space charge limited current (SCLC), providing a direct measure of mobility as a function of temperature and field. The average electron mobility for this copolymer was 0.85 $\times$ 10^{-2} cm^2/Vs. The photogeneration mechanism in blends of copolymer **P** (electron acceptor) with poly(3-phenyl hydrazone thiophene) (PPHT) (electron donor) were investigated. Annealing of the complete device was found to result in an increase in power conversion efficiency from 1.67% to 2.32%. By studying the dependence of photocurrent on effective bias voltage, annealing was found to increase the charge generation efficiency through an increase in the efficiency of separation of exciton following the charge transfer.

Introduction

Polymer solar cells (PSCs) have been extensively studied because of their motivation for developing inexpensive, efficient, and renewable energy sources.[1−4] Power conversion efficiencies (PCEs) as high as 5−6% have been reported for bulk heterojunction PSCs using regioregular poly(3-hexylthiophene) (P3HT) as donor and a solution processable fullerene derivative (PCBM) as acceptor.[5,6] However, there are some drawbacks of PCBM for application in PSCs, including weak absorption in the visible region and the possibility of phase separation from the polymer donor. Therefore, nonfullerene hybrid devices[7,8] and PSCs in which a polymer donor is blended with a polymer acceptor have attracted interest recently.[9−14] However, the PCE of polymer devices remains relatively low at present. One of the reasons for the low efficiency of the PSCs is the lack of good polymer acceptors with high electron affinity, high electron mobility, and good sunlight-harvesting properties. The peak photon intensity of the solar spectrum lies at about 700 nm. To make the absorption spectra of the conjugated polymers match the solar spectrum, their absorption maximum should be near 700 nm, which means that the band gap (E_g) of the conjugated polymer should be lower than 1.74 eV.[15] The most successful approach to obtain the low band gap polymers is a copolymerized D−A structure.[16−19] The copolymerization of the donor (electron−rich) with higher HOMO energy level and the acceptor (electron deficient) with lower LUMO energy level results in a lower band gap polymer due to an interchain charge transfer from donor to acceptor.

Perylene bisimides have attracted much interest and been widely investigated because of their unique merits such as thermal stability, inexpensiveness, and especially its large molar absorption coefficient and good electron accepting properties. They are potential candidates as electron-accepting materials in organic photovoltaic solar cells.[20] Both PPV and perylene bisimide chromophores have been applied in bulk-heterojunction-like solar cell configurations as donor and as acceptor materials, respectively.[21,22] Recently, a new class of donor−acceptor polymers consisting of alternating oligo(*p*-phenylenevinylene) and perylene bisimide connected via saturated spacers was synthesized.[23] Moreover, two copolymers containing perylene bisimide, PPV and triphenylamine segments were synthesized and used for photovoltaic cells.[24] Finally, a series of novel alternating phenylenevinylene or fluorenevinylene copolymers containing perylene bisimide were synthesized in our laboratory and were used for photovoltaic cells.[25]

The main objective of the present investigation was the synthesis and characterization of an alternating phenylenevinylene copolymer containing perylene bisimide moieties that is a candidate for photovoltaic cells. This copolymer was successfully synthesized by Heck coupling and had the donor (D)−acceptor (A) architecture. In particular, it contained the electron-donating 2,5-dihexyloxyphenylene as the D unit and the electron-withdrawing perylene bisimide as the A unit. The alternating copolymerization of D and A units has been used as an effective way to lower the band gap of conjugated

* Corresponding authors. E-mail: mikroyan@chemistry.upatras.gr (J.A.M.); sharmagd_in@yahoo.com (G.D.S.). Phone: +30 2610 997115 (J.A.M.); +91-0291-2720857 (G.D.S.). Fax: +30 2610 997118 (J.A.M.); 91-0291-2720856 (G.D.S.).

† Chemical Technology Laboratory, Department of Chemistry, University of Patras.

‡ Physics Department, Molecular Electronic and Optoelectronic, JNV University.

§ Defence Laboratory.

10.1021/jp901651z CCC: $40.75
Published on Web 04/14/2009

polymers. The photophysical, electrochemical, electrical, and photovoltaic properties of this copolymer were systematically studied and correlated with its chemical structure.

Experimental Section

Characterization Methods. IR spectra were recorded on a Perkin-Elmer 16PC FT-IR spectrometer with KBr pellets. ^{1}H NMR (400 MHz) spectra were obtained using a Bruker spectrometer. Chemical shifts (δ values) are given in parts per million with tetramethylsilane as an internal standard. Micromass Platform LC was used for mass spectroscopy. UV−vis spectra were recorded on a Bekman DU-640 spectrometer with spectrograde THF. The PL spectra were obtained with a Perkin-Elmer LS45 luminescence spectrometer. The PL spectra were recorded with the corresponding excitation maximum as the excitation wavelength. TGA was performed on a DuPont 990 thermal analyzer system. Ground samples of about 10 mg each were examined by TGA and the weight loss comparisons were made between comparable specimens. Dynamic TGA measurements were made at a heating rate of 20 °C/min in atmospheres of N_2 at a flow rate of 60 cm^3/min. Thermomechanical analysis (TMA) was recorded on a DuPont 943 TMA using a loaded penetration probe at a scan rate of 20 °C/min in N_2 with a flow rate of 60 cm^3/min. The TMA experiments were conducted at least in duplicate to ensure the accuracy of the results. The TMA specimens were pellets of 10 mm diameter and ∼1 mm thickness prepared by pressing powder of sample for 3 min under 8 kp/cm^2 at ambient temperature. The T_g is assigned by the first inflection point in the TMA curve, and it was obtained from the onset temperature of this transition during the second heating. Elemental analyses were carried out with a Carlo Erba model EA1108 analyzer.

The cyclic voltammetry (CV) of copolymer **P** was performed using a potentiostat−galvanostat (PGSTAT 30, Autolab, Eco-Chemie, Netherlands) employing a three-electrode cell at room temperature. The three electrode cell was comprised of a gold working electrode, a platinum (Pt) counter electrode, and a SCE reference electrode, calibrated against Fc/Fc+ couple (+0.470 V vs SCE) It was conducted in a distilled tetrahydrofuran (THF) solution containing the polymer and 0.1 M KCl as supporting electrolyte at a scan rate of 50 mV/s.

Reagents and Solvents. *N*,*N*-Dimethylformamide (DMF) and tetrahydrofuran (THF) were dried by distillation over CaH_2. Triethylamine was purified by distillation over KOH. All other reagents and solvents were commercially purchased and were used as supplied.

Preparation of Monomers and Polymer. ***1,7-Dibromo-3,4,9,10-perylenetetracarboxylic dianhydride (1).*** Compound **1** was prepared by bromination of 3,4,9,10-perylenetetracarboxylic dianhydride by means of bromine and a catalytic amount of iodine in sulfuric acid according to the literature.[26] The 1,7-dibromo derivative was the predominant isomer, which was obtained as reaction product.

1,7-Bis(4-tert-butylphenoxy)perylene-3,4:9,10-tetracarboxylic Acid Dianhydride (2). Compound **2** was prepared from the reaction of **1** with 4-*tert*-butylphenol in DMF in the presence of K_2CO_3.[26]

1,7-Bis(4-tert-butylphenoxy)perylene-3,4:9,10-tetracarboxylic-bis(p-bromophenylimide) (3). A flask was charged with a mixture of **2** (0.1740 g, 0.253 mmol), 4-bromoaniline (0.1347 g, 0.783 mmol), DMF (30 mL), and glacial acetic acid (0.07 g, 1.16 mmol). The mixture was stirred and refluxed for 18 h under N_2. It was subsequently concentrated under reduced pressure. The concentrate was poured into water (∼100 mL) containing hydrochloric acid 35% (3 mL). The precipitate was filtered, washed with water, and dried to afford **3** (0.2227 g, yield 88%).

Anal. Calcd for $C_{56}H_{40}Br_2N_2O_6$: C, 67.48; H, 4.04; N, 2.81. Found: C, 66.14; H, 4.12; N, 3.17.

FT-IR (KBr, cm^{-1}): 3058, 1704, 1672, 1592, 1506, 1488, 1402, 1340, 1262, 1212, 1174, 1072, 1012, 828, 514.

^{1}H NMR ($CDCl_3$, ppm): 8.63−7.66 (br, 6H, perylene protons); 7.25−7.53 (m, 12H, phenyl protons); 6.80 (m, 4H, phenyl protons ortho to oxygen); 1.35 (s, 18H, aliphatic protons).

Mass spectrometry (MS) (electrospray: 30 eV): (M + 1) 997.73.

1,4-Divinyl-2,5-bis(hexyloxy)-benzene (4). Compound **4** was prepared by Stille coupling reaction[28] of 1,4-dibromo-2,5-bis(hexyloxy)-benzene with tributylvinyltin.[29]

Copolymer P. A flask was charged with a mixture of **3** (0.1140 g, 0.165 mmol), **4** (0.0547 g, 0.165 mmol), $Pd(OAc)_2$ (0.0015 g, 0.007 mmol), P(*o*-tolyl)$_3$ (0.0116 g, 0.038 mmol), DMF (8 mL), and triethylamine (3 mL). The flask was degassed and purged with N_2. The mixture was heated at 90 °C for 24 h under N_2. Then it was filtered and the filtrate was poured into methanol. The precipitate was filtered and washed with methanol. The crude product was purified by dissolving in THF and precipitating into methanol (0.0860 g, yield 60%).

Anal. Calcd for $(C_{78}H_{72}N_2O_8)_n$: C, 80.39; H, 6.23; N, 2.40. Found: C, 79.53; H, 6.16; N, 2.35.

FT-IR (KBr, cm^{-1}) (Figure 1): 3058, 2954, 2928, 2864, 1702, 1672, 1592, 1542, 1508, 1490, 1458, 1406, 1340, 1262, 1210, 1176, 1014, 970, 836, 544.

^{1}H NMR ($CDCl_3$, ppm) (Figure 2): 8.65−7.68 (br, 6H, aromatic "h"); 7.45 (m, 12H, aromatic "g"); 7.09 (m, 4H, olefinic "f"); 6.77 (m, 6H, aromatic "e"); 3.98 (m, 4H, aliphatic "d"); 1.82 (m, 4H, aliphatic "c"); 1.36 (m, 30H, aliphatic "b"); 0.93 (t, J = 6.1 Hz, 6H, aliphatic "a").

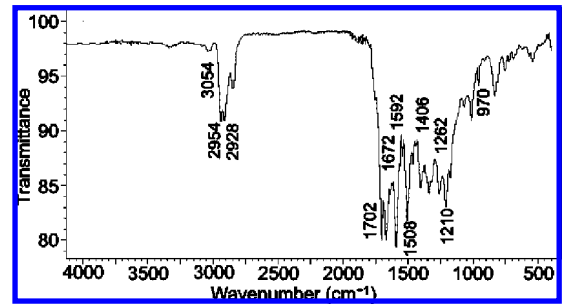

Figure 1. FT-IR spectrum of copolymer **P**.

Device Fabrication and Characterization. All the solar cell devices were fabricated in a sandwich geometry consisting of bottom indium tin oxide (ITO) coated electrode, a polymer thin film, and a top metal (Al) electrode. The ITO coated glass substrates were cleaned and dried prior to the device fabrication. The composite layers of 1:1 wt % PPHT:copolymer **P** were spin-coated on ITO-coated glass and then dried. The THF was used as solvent. To complete the solar cell devices, semitransparent Al electrode of thickness 10 nm electrode was deposited by thermal evaporation on the top of composite layer, at a vacuum of less than 10^{-5} Torr. The resultant active area of the devices was approximately 0.05 cm^2. The current−voltage characteristics under illumination and dark were obtained with a Keithley electrometer. A white light halogen lamp, calibrated to approximately 1.15 Sun (30 mW/cm^2) with a Si diode, was used as light source for the photoresponse measurements. The incident photon to current efficiency (IPCE) has been estimated from the following expression

$$\mathrm{IPCE} = 1240 J_{Sc}/\lambda P_{in} \quad (1)$$

where J_{sc} is the short circuit photocurrent and λ and P_{in} are the wavelength and illumination intensity of the incident light, respectively.

Results and Discussion

Synthesis and Characterization. Scheme 1 outlines the preparation of compounds **1**,[26] **2**,[27] **3**, and copolymer **P**. Compound **3** has not been previously prepared, and its synthesis was achieved from the reaction of **2** with excess of 4-bromoaniline in DMF in the presence of acetic acid. It was characterized by FT-IR and ^{1}H NMR spectroscopy (see Experimental Section). Copolymer **P** was prepared by Heck[30] coupling of **3** with **4** in DMF utilizing triethylamine as the proton scavenger and $Pd(OAc)_2$ as the catalyst. The crude product was purified by dissolution in THF and precipitation into methanol. The copolymer was obtained in 60% yield and had number average molecular weight (M_n) 7800, by GPC, with a polydispersity of 2.4 (Table 1). It was soluble in THF, chloroform, and other common organic solvents due to the *tert*-butyl and hexyloxy side groups.

The FT-IR spectrum of **P** (Figure 1) showed characteristic absorption bands at 3054, 1592, 1508 (aromatic); 1702, 1672 (imide structure); 2954, 2928 (C−H stretching of aliphatic chains); 1406 (C−H deformation of −C-$(CH_3)_3$); 1262, 1210 (ether bond). The ^{1}H NMR spectrum of **P** (Figure 2) displayed a broad upfield signal at 8.65−7.68 ppm assigned to the six perylene protons "h". The aromatic protons "g" and "e" and the olefinic protons "f" gave multiplets at 7.45, 6.77, and 7.09 ppm, respectively. Finally, the aliphatic protons "a", "b", "c", and "d" resonated at 0.93, 1.36, 1.82, and 3.98 ppm, respectively.

Figure 3 presents the TGA and TMA traces of **P** in N_2, while all thermal characteristics are summarized in Table 1. It was stable up to about 300 °C, had decomposition temperature (T_d) that corresponds to 5% weight loss of 370 °C, and char yield (Y_c) of 49% at 800 °C. The TMA trace showed a distinguishable step from the onset of which the glass transition temperature (T_g) was determined to be 72 °C. The relatively high fraction of the aliphatic segments in the molecule of **P** suppressed its rigidity.

Photophysical Properties. Figure 4 presents the normalized UV−vis spectra of **P** in dilute (10^{-5} M) THF solution and thin

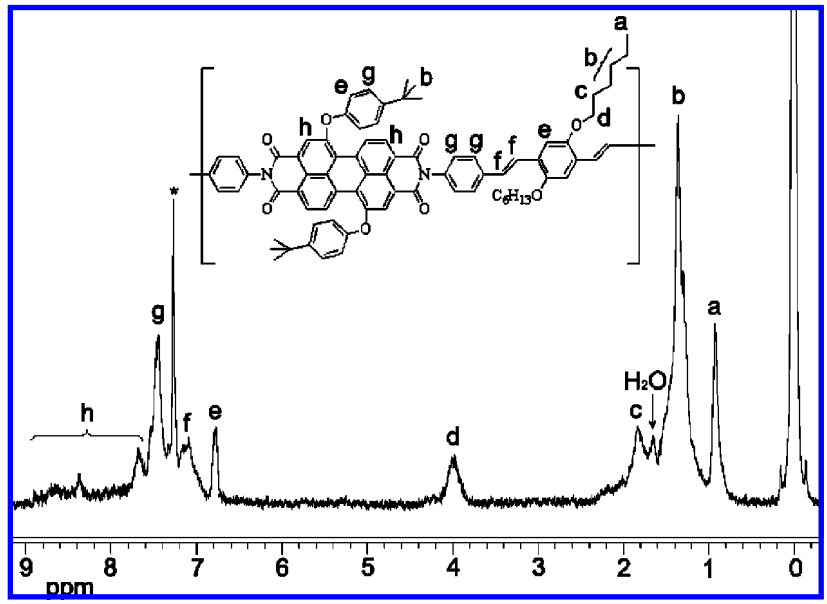

Figure 2. ^{1}H NMR spectrum in $CDCl_3$ solution of copolymer **P**. The solvent peak is denoted by an asterisk.

SCHEME 1: Synthesis of Compounds 1−3 and Copolymer P

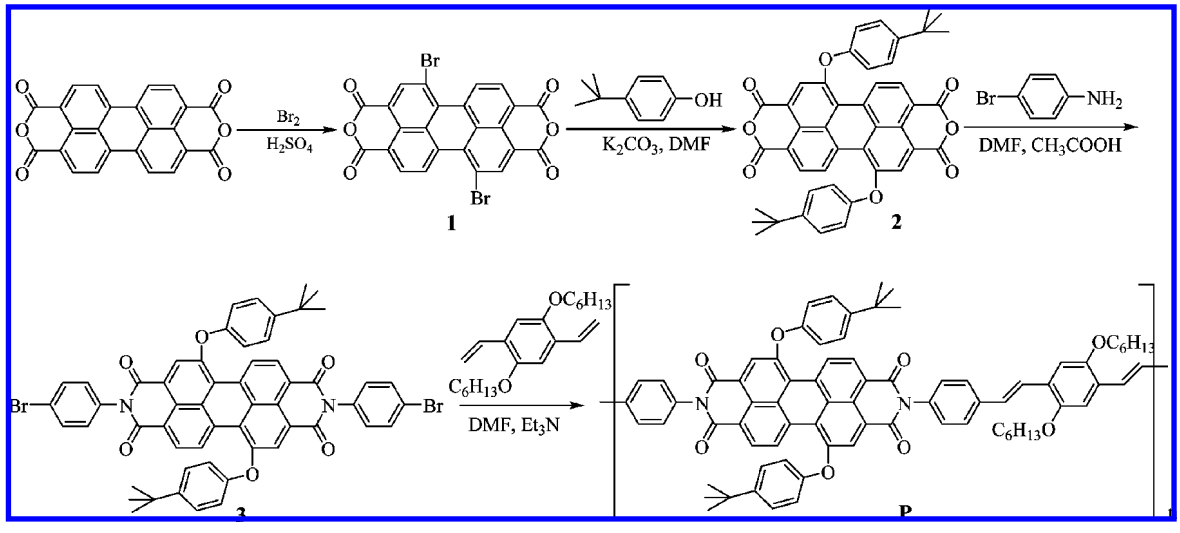

TABLE 1: Molecular Weights, Thermal, Optical, and Electrochemical Properties of copolymer P[a]

M_n[b]	M_w/M_n[b]	T_d[c] (°C)	Y_c[d] (%)	T_g[e] (°C)	$\lambda_{a,max}$[f] in solution (nm)	$\lambda_{f,max}$[g] in solution (nm)	$\lambda_{a,max}$[f] in thin film (nm)	E_g^{opt}[h] (eV)	HOMO (eV)	LUMO (eV)	$E_{g(electro)}$[j]
7800	2.4	370	49	72	500	555	504	1.66(748 nm)[i]	−5.75	−3.95	1.76

[a] The PL emission spectra were recorded at 480 nm excitation wavelength. [b] Molecular weights determined by GPC using polystyrene standard. [c] Decomposition temperature corresponding to 5% weight loss in N_2 determined by TGA. [d] Char yield at 800 °C in N_2 determined by TGA. [e] Glass transition temperature determined by TMA. [f] $\lambda_{a,max}$: the absorption maxima from the UV−vis spectra in THF solution or in thin film. [g] $\lambda_{f,max}$: the PL maxima in THF solution. [h] E_g: The optical band gap calculated from the onset of thin film absorption spectrum. [i] Number in parentheses indicates the onset of thin film absorption spectrum. [j] The electrochemical band gap.

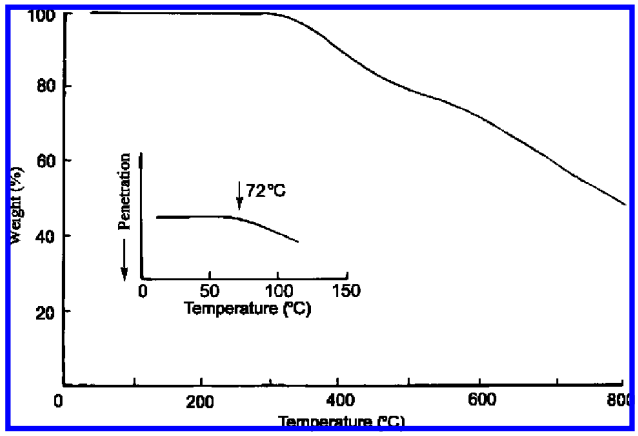

Figure 3. TGA thermogram of copolymer **P** in N_2. The insert shows the TMA trace of this copolymer. Conditions: N_2 flow, 60 cm^3/min; heating rate, 20 °C/min.

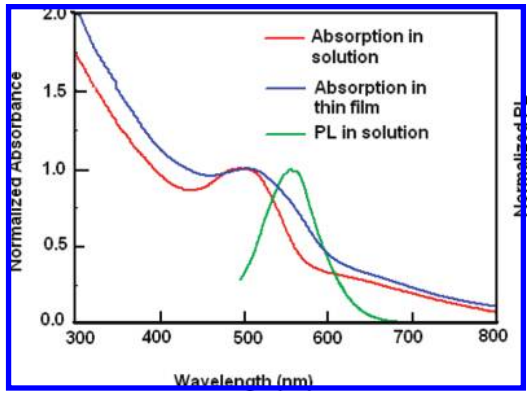

Figure 4. Normalized UV−vis absorption spectra of copolymer **P** in THF solution and thin film as well as PL emission spectrum of this copolymer in THF solution. The PL emission spectrum was obtained by photoexcitation at 480 nm.

film as well as the PL emission spectrum in THF solution. All photophysical properties are listed in Table 1. Because the thin film of **P** was not photoluminescent to a detectable extent, its PL spectrum could not be recorded. Quenching of the emission of copolymer thin film indicated interaction and charge/energy transfer from the phenylenevinylene to the perylene bisimide.[31] The absorption spectra (Figure 4) were broad and extended up to about 800 nm, with longer wavelength maximum at ∼500 nm. It seems that the absorption spectrum of thin film was broader than that of solution and showed an absorption onset at 748 nm that corresponds to an optical band gap (E_g^{opt}) of 1.66 eV. This E_g^{opt} is significantly lower than that (2.10 eV) of 2-methoxy-5-(2-ethylhexyloxy)-1,4-phenylenevinylene (MEH-PPV).[32] An E_g^{opt} value of about 2.0 eV has been reported for donor−acceptor type thiophene−perylene−thiophene polymers.[27] Moreover, oligothiophene-functionalized perylene bisimide systems have displayed E_g^{opt} of 1.97−1.63 eV.[31] Finally,

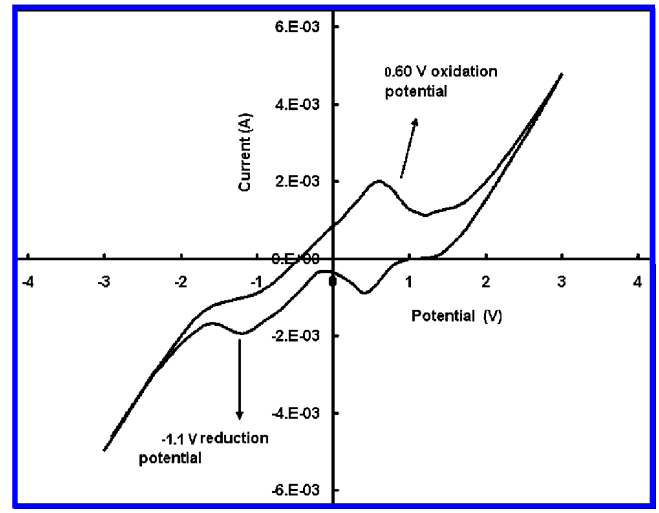

Figure 5. Cyclic voltammetry of copolymer **P**.

other related perylene−phenylenevinylene copolymers[25] displayed comparable E_g^{opt} values of 1.55−1.56 eV.

The solution of **P** emitted yellow−orange light with PL maximum at 555 nm when it was photoexcited at 480 nm (Figure 4).

The highest occupied molecular orbital (HOMO) and lowest unoccupied molecular energy orbital (LUMO) energy level of copolymer **P** were measured by cyclic voltammetry as shown in Figure 5. The values of E_{HOMO} and E_{LUMO} estimated from the oxidation potential and reduction potential are −5.75 and −3.95 eV, respectively. The electrochemical energy band gap, i.e., $E_{g(electro)} = E_{HOMO} - E_{LUMO}$ estimated is 1.76 eV, which is very close to the value measured from the optical absorption spectra (Table 1). Similar electron affinity about 3.9 eV was reported for a polymer acceptor based on alternating dithienothiophene and perylene diimide units.[18] The low band gap observed in this copolymer is due to the electron-donating 2,5-dihexyloxyphenylene as the D unit and the electron-withdrawing perylene bisimide as the A unit. Moreover, the electron affinity with a LUMO energy level −3.9 eV (similar to the LUMO level of PCBM) can be used as an electron acceptor for polymer−polymer bulk heterojunction photovoltaic device.

Electrical Properties of Copolymer P. The $J-V$ characteristics of ITO/copolymer **P**/Al device in dark and under illumination are shown in Figure 6. In these characteristics, the forward bias corresponds to the positive and negative voltage applied to Al and ITO electrode, respectively. The $J-V$ characteristics show asymmetrical and exhibit rectification. This behavior can be explained by small work function of Al electrode and n type semiconductivity of polymer layer. The rectification effect observed in this device is due to the formation of a Schottky barrier at ITO−polymer and Ohmic contact with Al electrode. In the present device, the Fermi level of the Al (−4.1 eV) matches closely to the LUMO level of copolymer **P** and indicates the formation of Ohmic contact for electron injection

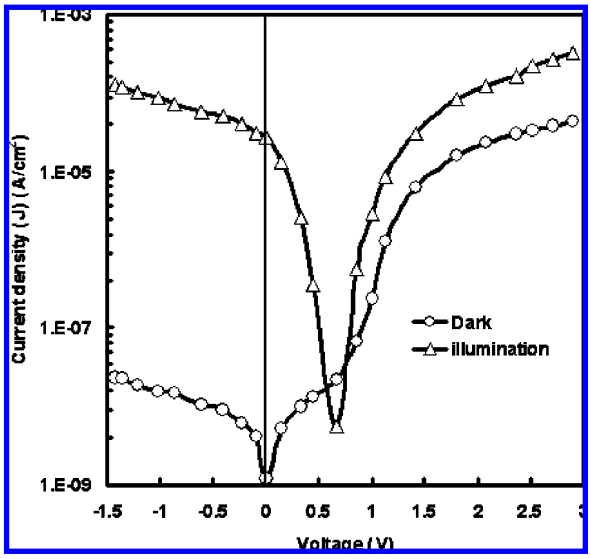

Figure 6. Current−voltage characteristics of ITO/copolymer **P**/Al device in dark and under illumination.

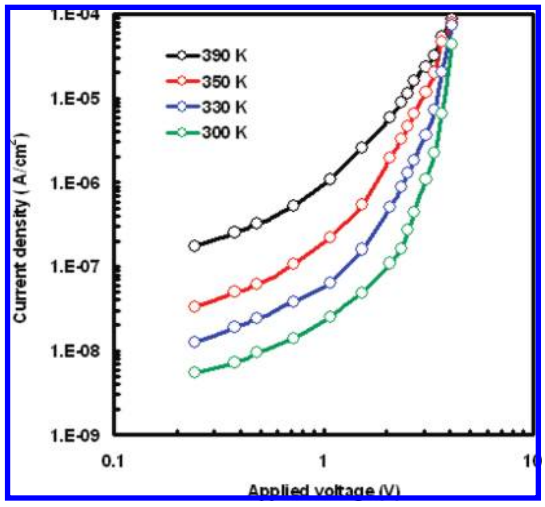

Figure 7. Current−voltage characteristics for ITO/copolymer **P**/Al device in dark at different temperatures.

from Al electrode, whereas the ITO form the Schottky barrier with copolymer **P**, which is responsible for rectification effect.

The photovoltaic device based on this polymer exhibits an open circuit voltage 0.69 V, a short circuit current 0.027 mA/cm^2, fill factor 0.34, and overall power conversion efficiency about 0.018%. This has been improved when this copolymer is used as an electron acceptor in a bulk heterojunction device with an electron donor conjugated polymer. This is discussed in more detail in the last part of the discussion section.

Space charge limited current (SCLC) measurements have been used to evaluate carrier mobility under steady state of current in organic layer.[33−35] We have applied the SCLC method to evaluate the electron mobility of electron transporting polymer. We have fabricated the electron only device with structure of ITO/copolymer **P**/Al. Figure 7 shows the current density−voltage characteristics log−log scale at different temperature ranging from 300−390 K. It was observed that below a bias voltage 2.0 V, the current density in the entire temperature range, varies in accordance with the relation for space charge limited conduction[36] for trap free polymer material and the current density is given by

$$J = \frac{9}{8}\varepsilon\varepsilon_o\mu(0)\frac{E^2}{L} \quad (2)$$

where E is the electric field, ε and ε_o are the relative dielectric constant and the permittivity of the free space, respectively, L is the thickness of the organic layer, and $\mu(0)$ denotes the mobility of charge carriers at fields tending to zero. The relative dielectric constant is assumed to be 3.5 for polymer and the permittivity of the free space $\varepsilon_o = 8.85 \times 10^{-12}$ F/m, the low field mobility is calculated as a function of temperature. The variation of low field mobility with temperature is shown in Figure 8. It is found that the mobility is thermally activated in accordance with the relation

$$\mu(0) = \mu_0 \exp(-\Delta/kT) \quad (3)$$

where μ_0 is the pre-exponential factor and Δ is the thermal activation energy. The thermal activation energy and pre-exponential factor is calculated to be 0.31 eV and 4.56×10^{-2} cm^2/Vs, respectively. The value of activation energy for a large number of disordered molecular materials has been found vary between 0.4 and 0.6 eV.[37] In the nonhomogeneous conjugated polymers, the crystalline conjugated systems are connected in series by amorphous regions. The polaron energy of the ordered segments varies with the conjugation length of the segment (lower polaron energy for higher conjugation length). The mobility activation energy represents the variation in the average energy of the adjacent hopping sites for the polarons. The charge transport occurs by tunneling of hopping between adjacent sites through the disordered regions, which creates a potential barrier for the mobility of the carrier. The value of thermal activation energy for the copolymer **P** is lower than the above values. This could be due to the fact that amorphous regions in these films are much smaller in size as compared to the crystalline regions, resulting in a lower potential barrier.

It is observed that for bias voltages higher than 2.0 V, the current density (J) is larger than expected from eq 2. The carrier mobility is affected by the energetic disorder due to the interaction of each hopping charge with randomly oriented and randomly located dipoles in the organic thin films.[36] At any temperature, the high field and the mobility is dependent on the electric field and can be expressed by a Poole−Frenkel (PF) equation:

$$\mu(E) = \mu(0) \exp(\beta\sqrt{E}) \quad (4)$$

where μ (0) is the zero field mobility and β is the Poole−Frenkel factor, which depends on the interaction between the charge

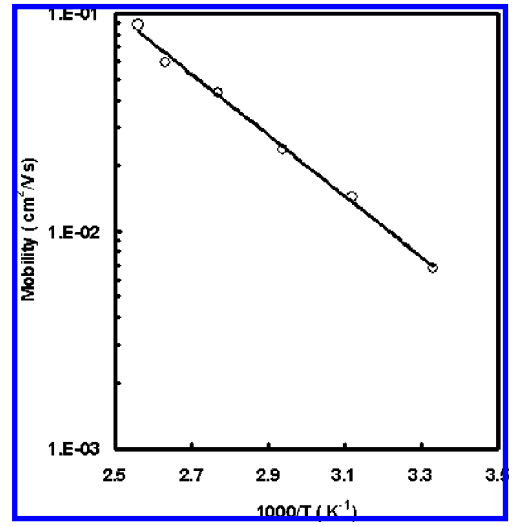

Figure 8. Temperature dependent on low field electron mobility for copolymer **P** estimated from SCLC data.

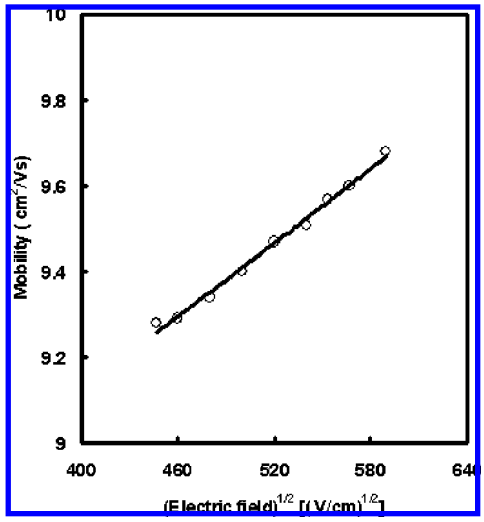

Figure 9. Electric field variation of mobility at room temperature.

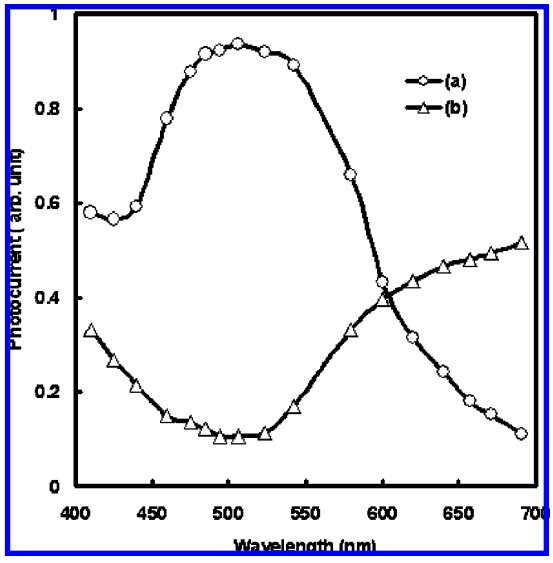

Figure 10. Action spectra of photocurrent of the ITO/copolymer **P**/Al device, illuminating through (a) ITO side and (b) Al side.

carriers and the randomly distributed permanent dipoles in the semidconducting polymers.[36] For room temperature measurements, the variation of $\mu(E)$ with $E^{1/2}$ is shown in Figure 9. The intercept on mobility axis and slope gives the value of zero field mobility and Poole−Frenkel factor, which are 0.85×10^{-2} cm^2/Vs and 3.0×10^{-4} $(cm/V)^{1/2}$, respectively. The electric field helps the hopping carriers to overcome the potential barrier, resulting in an increase in the value of mobility with the increase in electric field. The average value of electron mobility for copolymer **P** is estimated about 0.85×10^{-2} cm^{-2}/Vs, This value of mobility is very close to the reported for conjugated polymer having similar chemical structure measured from field effect transistor measurements[18,38] and higher than that for cyano substituted PPV.[39]

Curves a and b in Figure 10 show the action spectra of photocurrent for the device ITO/copolymer/Al device, illuminating through Al and ITO side, respectively. The shape action spectra of the device, illuminating through the ITO side are similar to the absorption spectra of polymer thin film. This indicates that the carrier generation that occurs via excitation of polymer film is in proportion to the absorbance. On the other hand, the action spectra of the device, illuminating through the Al side, are quite different from the absorption spectra of the

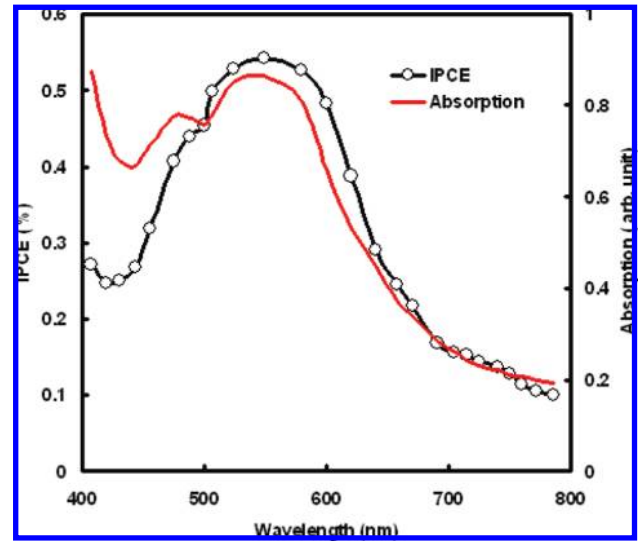

Figure 11. IPCE spectra of copolymer solar cell at illuminated intensity 30 mW/cm^2 along with the absorption spectra of the blend.

polymer. This indicates that the photocarriers are generated via exciton dissociate dominantly at the Schottky barrier formed at ITO−polymer interface. When the device is illuminated through the Al side, the incident light is absorbed in the bulk region, before reaching the depletion layer. Excitons that are generated in the bulk are lost during their transportation toward the Schottky barrier before dissociation.

From the above results, we conclude that this copolymer behaves as an n type organic semiconductor with average electron mobility 0.85×10^{-2} cm^{-2}/Vs, which form an Ohmic contact and Schottky barrier with high work function ITO electrode and low work function Al electrode, respectively. The generation of photocarrier in this device is due to the dissociation of excitons into free charge carriers due to the built-in field at the ITO−copolymer interface. This copolymer can be used as an electron acceptor of bulk heterojunction photoactive device.

Photovoltaic Properties of Bulk Heterojunction. To investigate the potential of polymer for photovoltaic application, we have used copolymer **P** as an acceptor and poly(3-phenyl hydrazone thiophene) (PPHT), the synthesis and photovoltaic properties of which have been previously reported[40] as an electron donor, and fabricated all polymer solar cell with structure ITO/PPHT:**P** (1:1 w/w)/Al. The IPCE spectra of the photovoltaic device along with the absorption spectra of the blend are shown in Figure 11. The absorption spectra of the blend exhibit a very broad absorption band between 400 and 800 nm and a broad incident photon to current conversion efficiency with maximum at 550 nm. The IPCE spectra characteristics of the solar cell show the main peak at about 550 nm and a shoulder at approximately 480 nm, corresponding to the absorption maxima of the donor polymer. The current−voltage characteristics of the photovoltaic device in dark and under illumination of white light (intensity of 30 mW/cm^2) based on the blend of electron donor and acceptor are shown in Figure 12. The curves show diode characteristics in dark. Under the illumination of white light calibrated to AM1.5 Sun intensity 30 mW/cm^2, the bulk heterojunction device exhibits an open circuit voltage (V_{oc}) of 0.65 V, a short circuit photocurrent (J_{sc}) of 2.14 mA/cm^2, fill factor (FF) of 0.36, and power conversion efficiency about 1.67% (Table 2). This value of power conversion efficiency is higher than that for the photovoltaic device with electron acceptor polymer, i.e., 0.085%. The overall power conversion efficiency of the device is further improved when

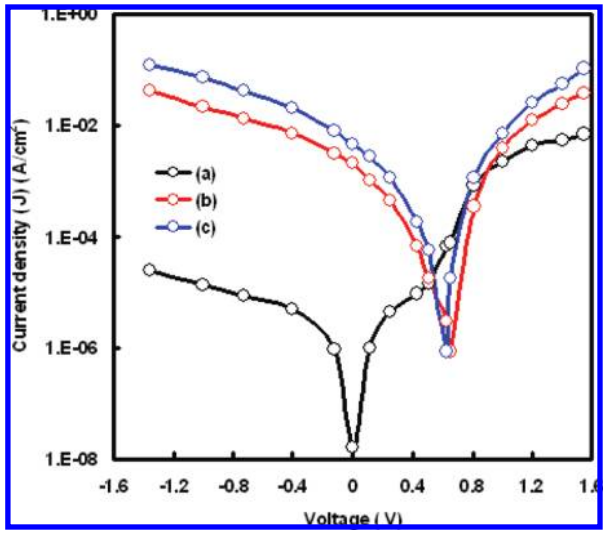

Figure 12. Current−voltage characteristics of the device in (a) dark, (b) illumination (unannealed), and (c) illumination (annealed at 80 °C for 10 min).

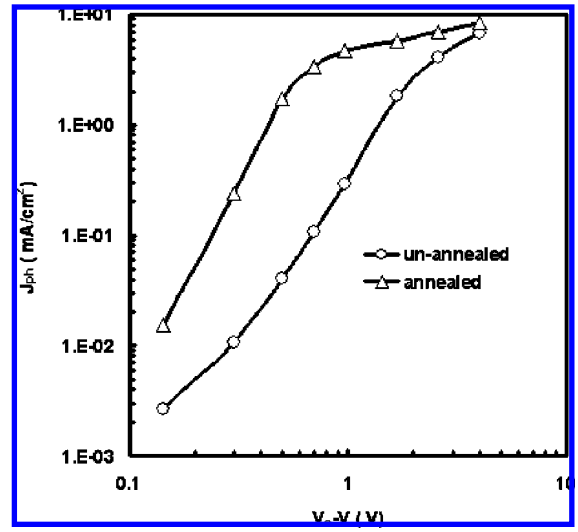

Figure 13. Dependence of photocurrent on effective applied voltage ($V_o - V$) under illumination of 30 mW/cm^2.

TABLE 2: Photovoltaic Parameters of the Devices Using as Photoactive Layer Blends of Poly(3-phenyl hydrazone thiophene) (PPHT) and Copolymer P

photoactive layer	J_{sc}[a] (mA/cm^2)	V_{oc}[b] (V)	FF[c]	PCE[d] (%)
PPHT: **P** (1:1 w/w) (unannealed)	2.14	0.65	0.36	1.67
PPHT: **P** (1:1 w/w) (annealed)	2.98	0.60	0.39	2.32

[a] J_{sc}: Short-circuits current density. [b] V_{oc}: Open-circuit voltage. [c] FF: Fill factor. [d] PCE: Power conversion efficiency.

the device is annealed at temperature of 80 °C for 10 min (Figure 12c), i.e., J_{sc} of 2.98 mA/cm^2, V_{oc} of 0.60 V, fill factor 0.39, and power conversion efficiency of 2.32% (Table 2). Similar power conversion efficiency of about 1.48% has been recently reported[41] for the BHJ photovoltaic devices based on a blend of copolymer of perylene diimide and bis(dithienothiophene) (as acceptor) and polythiophene derivative substituted by tris(thienylenevinylene) conjugated side chain measured under AM1.5 illumination of 100mW/cm^2. The PCE for our device is less than that reported for the regioregular MDMO-PPV: PCBM system (3.1%).[42] They have concluded that this improvement is attributed to both the fine mixing morphology of two components and the higher hole mobility of the films. However, the lower PCE in our device in comparison to the above device is basically limited by the low value of open circuit voltage and fill factor and random nature of PPHT. The low value of fill factor of the device is due to the electron traps present in copolymer P phase, which contributes to the recombination losses.

An all-polymer bulk heterojunction solar cell consists of a polymer blend sandwiched between two electrodes. The transparent indium tin oxide (ITO) forms an Ohmic contact for the holes. For electrons, Al forms an Ohmic contact with lowest unoccupied molecular orbital (LUMO) of the electron acceptor copolymer. An exciton generated in the donor and/or acceptor phase can diffuse toward the interface between two polymers. Subsequently, electrons transfer to the acceptor (hole transfer to the donor) occurs because of the difference in electron affinities and ionization potential of the two polymers. In this way, a bound e−h pair is formed across the interface, with the hole in the donor polymer and the electron in the acceptor polymer. Because of the low dielectric constants of the organic materials, these e−h pairs are strongly bound by Coulomb interaction with binding energies typical of several tenths of electronvolt. This bound pair still needs to dissociate with the help of the internal electric field in the device in order to produce the free charge carriers, which are then transported to the appropriate electrodes. Figure 13 presents the reverse bias dependence of photocurrent (J_{ph}) for as spin-cast and annealed devices, measured by subtracting dark current−voltage curves from the respective current−voltage curves measured under illumination. J_{ph} is plotted as a function of the effective voltage across the device, $V_o - V$, where V_o is the compensation voltage defined as the voltage at which $J_{ph} = 0$.[43] Plotting J_{ph} in this way allows the better comparison of the dependence of photocurrent on reverse bias, particularly in devices with different open circuit voltages.[44] Most notable in the figure is the dramatic change in the shape of the photocurrent curves with thermal annealing. The as-cast device shows a near-linear dependence of photocurrent on effective voltage out of −2.0 V reverse bias, similar to what has been observed from other all polymer blends.[45,46] However, the annealed device exhibits a partially saturated regime with onset at a 0.5 V, similar to what was observed for photovoltaic devices with a polymer/ fullerene blend as a photoactive layer.[43] Furthermore, at low fields ($V_o - V < 0.1$ V), the annealed device shows a 3-fold increase in photocurrent generation compared to the unannealed device. This is attributed to the low dissociation efficiency of bound electron−hole pairs for an unannealed device;[45,47] the increase in photocurrent at low fields and partial saturation of photocurrent at higher fields points to a significant increase in the dissociation efficiency of bound electron−hole pairs in the annealed device. The observed convergence of photocurrent at high field upon thermal annealing confirms that the numbers of photogenerated excitons are comparable with the unannealed device. However, the exciton dissociation efficiency and charge collection efficiency improved significantly upon thermal annealing. Recent studies on devices based on polymer blends as photoactive have been accounted for the improvement in the device performance upon thermal annealing. This is due to the increase in the efficiency of exciton dissociation.[47−49]

After the photoinduced transfer at the donor/acceptor interfaces present in the bulk of photoactive layer in bulk heterojunction photovoltaic devices and subsequent dissociation, the

electrons are localized in the copolymer P phase, whereas the holes remain in the PPHT in the present device. Subsequently, the free electrons and holes must be transported via percolated copolymer P and PPHT pathways toward the Al and ITO electrodes, respectively, to produce the photocurrent. Therefore, the electron transport in copolymer P and hole transport in PPHT are crucial for the understanding of the photogeneration process in bulk heterojunction devices. For pure copolymer P, the electron mobility ($\mu_e = 0.85 \times 10^{-2}$ cm^2/Vs) was found to be 3.26×10^3 times higher than the hole mobility in pure PPHT ($\mu_h = 2.6 \times 10^{-6}$ cm^2/Vs). An important question is whether these mobilites are modified or not when the materials are blended as in the active layer of a photovoltaic device.

We have investigated the effect of thermal annealing on the performance of photovoltaics in terms of physical parameters such as the charge carrier mobility. To get information about the effect of thermal annealing on charge transport in the bulk heterojunction devices, we have measured the electron and hole mobility in the blended thin films, using electron only and hole only devices as reported earlier in literature for P3HT:PCBM blends.[50] To measure the SCLC of only one type of charge carrier in a blend, the other one must be suppressed by a large injection barrier, resulting in an electron or hole only device. We have measured the dark current density−voltage curves of PPHT:P blends for hole only and electron only devices for both devices using annealed and unannealed blend thin films. To fabricate the hole only device, gold (Au) was evaporated as the top electrode having structure ITO/PPHT:P/Au. The work function of ITO matches the HOMO level of PPHT, forming Ohmic contact with for hole injection, whereas the Au strongly suppress the electron injection into PCBM owing to the large mismatch between its workfunction and LUMO of PCBM. A schematic diagram of the hole only device is shown in the insert of Figure 14a. To suppress the hole injection into PPHT, the bottom electrode must have low work function. Therefore, we have fabricated an electron only device by sandwiching the PPHT:P blend between two Al electrodes as shown in the insert of Figure 14b. Parts a and b of Figure 14 show the experimental dark current densities (J_d) of PPHT:P blends that were measured in hole only and electron only devices for as cast and annealed blend films, respectively. We have observed that when the applied voltage is greater than built in potential (V_{bi}), the dark current scales quadratically with voltage, indicating SCL transport and dark current follow the following equation:[51]

$$J = \frac{9}{8}\varepsilon\mu_o\, e^{0.891\gamma\sqrt{V_{int}/L}}\frac{V_{int}^2}{L^3} \quad (5)$$

where μ_o is the zero field mobility, γ is the field activation parameter, ε is the dielectric constant, and L is the thickness of active layer and V_{int} is the internal voltage drop $V_{int} = V - V_{bi}$. V_{bi} is the built-in voltage that arises from the difference in work function between the bottom and top electrode. Fitting the experimental current−voltage characteristics for hole only and electron only device, the hole mobility and electron mobility were estimated for devices used with both an unannealed and an annealed blend layer. It is found that there is an increase in hole mobility (from 2.6×10^{-6} cm^2/Vs to 8.3×10^{-4} cm^2/Vs) for the annealed, whereas the electron mobility remains unaffected upon thermal annealing. Therefore, the most important factor that leads to an increase in PCE is the enhancement in hole mobility of PPHT in the blend by about two orders of magnitude. In a device with unannealed blended film, the difference in the electron and hole mobility is too large, and the photocurrent is strongly limited by the building of space charge. However, the difference in the electron and hole mobility is reduced in a device based on annealed blend film and the space charge no longer limits the photovoltaic performance of device due the more balance charge transport.

It is well-known that the mobility of polythiophene conjugated polymer is strongly influenced by the degree of intermolecular order. An improvement in PPHT hole mobility with annealing may contribute significantly to the efficiency improvement observed in the present investigation as predicted by device modeling of Marsh et al.[52] We conclude that the increase in the efficiency of the present solar cells upon thermal annealing is attributed to the large increase in hole mobility as a result of improved crystallinity. The significant increase in hole mobility upon thermal annealing provides an explanation for the increase in the charge collection efficiency. An increase in phase separation with thermal annealing may also contribute to the increase in the exciton dissociation efficiency.

The fill factor of the device also improves upon the thermal annealing. Marsh et al.[52] have also shown that when the exciton dissociation efficiency is improved through an increase in mobility, both charge collection efficiency and fill factor are improved, whereas only carrier collection efficiency is improved through a reduction in exciton recombination alone. Thus the

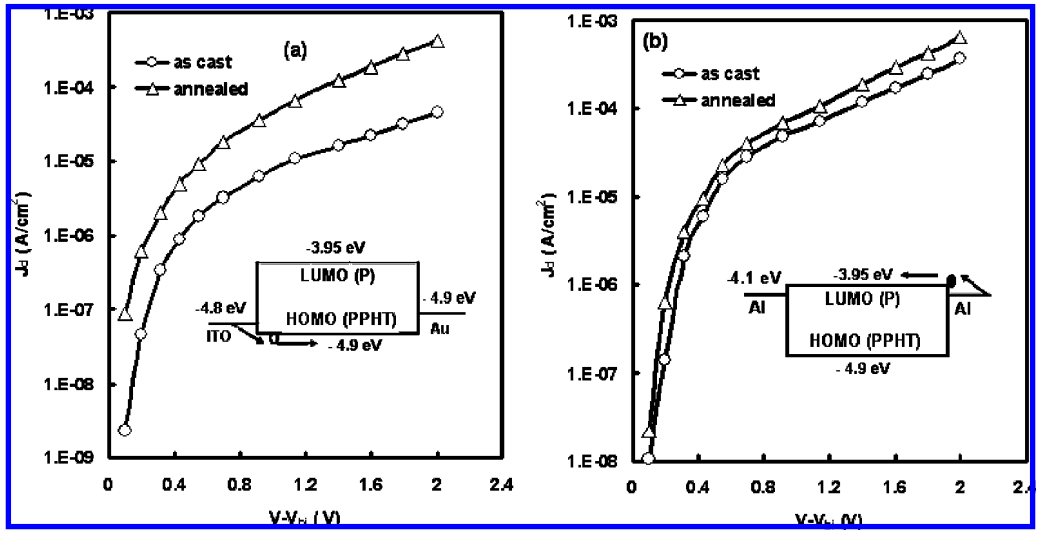

Figure 14. Experimental dark current densities of PPHT:P blend devices in (a) hole only device and (b) electron only device configuration. Inset: schematic diagrams of the devices.

increased fill factor in the annealed device may be attributed to the increase in hole mobility.

Conclusions

The Heck reaction of 1,4-divinyl-2,5-bis(hexyloxy)-benzene with a dibromide **3** afforded the soluble alternating copolymer **P**. The absorption of **P** was broad and extended up to about 800 nm with a longer wavelength maximum around 500 nm and an optical band gap of 1.66 eV. The solution of **P** emitted yellow−orange light with maximum at 555 nm. Quenching of the emission in thin film of **P** was observed, suggesting interaction and charge/energy transfer from the phenylenevinylene to the perylene bisimide. The current−voltage characteristics of the device based on this copolymer indicate that this behaves as an electron acceptor. The photovoltaic device based on the bulk heterojunction with PPHT shows a power conversion efficiency of 1.67%, which is further improved up to 2.32% upon thermal annealing. The enhancement in the power conversion efficiency upon thermal annealing attributed to the more balanced charge transport in the device as compared to that for a device employing unannealed blend film.

References and Notes

(1) Yu, G.; Gao, J.; Hummelen, J. C.; Wudl, F.; Heeger, A. J. *Science* **1995**, *270*, 1789.
(2) Gunes, S.; Neugebauer, H.; Sariciftci, N. S. *Chem. Rev.* **2007**, *107*, 1324.
(3) Winder, C.; Sariciftci, N. S. *J. Mater. Chem.* **2004**, *14*, 1077.
(4) Bundgaard, E.; Krebs, F. C. *Sol. Energy Mater. Sol. Cells* **2007**, *91*, 954.
(5) Kim, J. Y.; Lee, K.; Coates, N. E.; Moses, D.; Nguyen, T.-Q.; Dante, M.; Heeger, A. J. *Science* **2007**, *317*, 222.
(6) Li, G.; Shrotriya, V.; Huang, J.; Yao, Y.; Moriarty, T.; Emery, K.; Yang, Y. *Nat. Mater.* **2005**, *4*, 864.
(7) Krebs, F. C. *Sol. Energy Mater. Sol. Cells* **2008**, *92*, 715.
(8) White, M. S.; Olson, D. C.; Shaheen, S. E.; Kopidakis, N.; Ginley, D. S. *Appl. Phys. Lett.* **2006**, *89*, 143517/1.
(9) Halls, J. J. M.; Walsh, C. A.; Greenham, N. C.; Marseglia, E. A.; Friend, R. H.; Moratti, S. C.; Holmes, A. B. *Nature (London)* **1995**, *376*, 498.
(10) Arias, A. C.; MacKenzie, J. D.; Stevenson, R.; Halls, J. J. M.; Inbasekaran, M.; Woo, E.; Richards, P. D.; Friend, R. H. *Macromolecules* **2001**, *34*, 6005.
(11) Kim, Y.; Cook, S.; Choulis, S. A.; Nelson, J.; Durrant, J. R.; Bradley, D. D. C. *Chem. Mater.* **2004**, *16*, 4812.
(12) Veenstra, S. C.; Verhees, W. J. H.; Kroon, J. M.; Koetse, M. M.; Sweelssen, J.; Bastiaansen, J. J. A. M.; Schoo, H. F. M.; Yang, X.; Alexeev, A.; Loos, J.; Schubert, U. S.; Wienk, M. M. *Chem. Mater.* **2004**, *16*, 2503.
(13) Breeze, A. J.; Schlesinger, Z.; Carter, S. A.; Tillmann, H.; Horhold, H.-H. *Sol. Energy Mater. Sol Cells* **2004**, *83*, 263.
(14) Kietzke, T.; Horhold, H.-H.; Neher, D. *Chem. Mater.* **2005**, *17*, 6532.
(15) Scharber, M. C.; Mühlbacher, D.; Koppe, M.; Denk, P.; Waldauf, C.; Heeger, A. J.; Brabec, C. J. *Adv. Mater.* **2006**, *18*, 789.
(16) Peet, J.; Kim, J. Y.; Coates, N. E.; Ma, W. L.; Moses, D.; Heeger, A. J.; Bazan, G. C. *Nat. Mater.* **2007**, *6*, 497.
(17) Wang, E. G.; Wang, L.; Lan, L. F.; Luo, C.; Zhuang, W. L.; Peng, J. B.; Cao, Y. *Appl. Phys. Lett.* **2008**, *92*, 033307/1.
(18) Zhan, X. W.; Tan, Z. A.; Domercq, B.; An, Z.; Zhang, X.; Barlow, S.; Y. Li, F.; Zhu, D. B.; Kippelen, B.; Marder, S. R. *J. Am. Chem. Soc.* **2007**, *129*, 7246.
(19) Huo, L. J.; He, C.; Han, M. F.; Zhou, E. J.; Li, Y. F. *J. Polym. Sci., Part A: Polym. Chem.* **2007**, *45*, 3861.
(20) Shin, A. W. S.; Jeong, H. H.; Kim, M. K.; Jin, S. H.; Lee, J. K.; Lee, J. W.; Gal, Y. S. *J. Mater. Chem.* **2006**, *16*, 384.
(21) Schenning, A. P. H. J.; Herrikhuyzen, J.; van Jonkheijm, P.; Chen, Z.; Würthner, F.; Meijer, E. W. *J. Am. Chem. Soc.* **2002**, *124*, 10252.
(22) Syamakumari, A.; Schenning, A. P. H. J.; Meijer, E. W. *Chem.—Eur. J.* **2002**, *8*, 3353.
(23) Neuteboom, E. E.; Meskers, S. C. J.; van Hal, P. A.; van Duren, J. K. J.; Meijer, E. W.; Janssen, R. A. J.; Dupin, H.; Pourtois, G.; Cornil, J.; Lazzaroni, R.; Brédas, J.-L.; Beljonne, D. *J. Am. Chem. Soc.* **2003**, *125*, 8625.
(24) Liu, Y.; Yang, C.; Li, Y.; Li, Y.; Wang, S.; Zhuang, J.; Liu, H.; Wang, N.; He, X.; Li, Y.; Zhu, D. *Macromolecules* **2005**, *38*, 716.
(25) Mikroyannidis, J. A.; Stylianakis, M. M.; Cheung, K. Y.; Fung, M. K.; Djurišić, A. B. submitted for publication.
(26) Würthner, F.; Stepanenko, V.; Chen, Z.; Saha-Möller, C. R.; Kocher, N.; Dietmar Stalke, D. *J. Org. Chem.* **2004**, *69*, 7933.
(27) Koyuncu, S.; Kus, M.; Demic, S.; Kaya, I.; Ozdemir, E.; Icli, S. *J. Polym. Sci., Part A: Polym. Chem.* **2008**, *46*, 1974.
(28) McKean, D. R.; Parrinello, G.; Renaldo, A. F.; Stille, J. K. *J. Org. Chem.* **1987**, *52*, 422.
(29) Peng, Q.; Li, M.; Tang, X.; Lu, S.; Peng, J.; Cao, Y. *J. Polym. Sci., Part A: Polym. Chem.* **2007**, *45*, 1632.
(30) Ziegler, C. B., Jr.; Heck, R. F. *Org. Chem* **1978**, *43*, 2941.
(31) Chen, S.; Liu, Y.; Qiu, W.; Sun, X.; Ma, Y.; Zhu, D. *Chem. Mater.* **2005**, *17*, 2208.
(32) Li, X.; Zhang, Y.; Yang, R.; Huang, J.; Yang, W.; Cao, Y. *J. Polym. Sci., Part A: Polym. Chem.* **2005**, *43*, 2325.
(33) Blom, P. W. M.; de Jong, M. J. M.; Vleggaar, J. J. M. *Appl. Phys. Lett.* **1996**, *68*, 3308.
(34) Bozano, L.; Carter, S. A.; Scott, J. C.; Malliaras, G. G.; Brock, P. *J. Appl. Phys. Lett.* **1999**, *74*, 1132.
(35) Yasuda, T.; Yamaguchi, Y.; Zou, D. C.; Tsutsui, T. *Jpn J. Appl. Phys., Part I* **2002**, *41*, 5626.
(36) Malliaras, G. G.; Salem, J. R.; Brock, P. J.; Scott, C. *Phys. Rev. B* **1998**, *58*, R13411.
(37) Pai, D. M. *J. Chem. Phys.* **1970**, *52*, 2285.
(38) Wong, W. Y.; Wang, X. Z.; He, Z.; Djurisic, A.; Yip, C. T.; Cheung, K. Y.; Wang, H.; Mak, C. K.; Chan, W. K. *Nat. Mater.* **2007**, *6*, 521.
(39) Chua, L. L.; Zaumseil, J.; Chang, J. F.; Ou, E. C. W.; Ho, P. K. H.; Sirringhaus, H.; Friend, R. H. *Nature (London)* **2005**, *434*, 194.
(40) Sharma, G. D.; Suresh, P.; Sharma, S. K.; Roy, M. S. *Sol. Energy Mater. Sol. Cells* **2008**, *92*, 61.
(41) Tan, Z.; Zhou, E.; Zhan, X.; Wang, X.; Li, Y.; Barlow, S.; Marder, S. R. *Appl. Phys. Lett.* **2008**, *93*, 073309 93.
(42) Tajima, K.; Suzuki, Y.; Hashimoto, K. *J. Phys. Chem. C* **2008**, *112*, 8507.
(43) Mihailetchi, V. D.; Koster, L. J. A.; Hummelen, J. C.; Blom, P. W. M. *Phys. Rev. Lett.* **2004**, *93*, 216601.
(44) Mihailetchi, V. D.; Koster, L. J. A.; Blom, P. W. M. *Appl. Phys. Lett.* **2004**, *85*, 970.
(45) Yin, C.; Kietzkle, T.; Neher, D.; Horhold, H. H. *Appl. Phys. Lett.* **2007**, *90*, 092117/1.
(46) Mandoc, M. M.; Veurman, W.; Koster, L. A. J.; de Boer, B.; Blom, P. W. M. *Adv. Funct. Mater.* **2007**, *12*, 2167.
(47) Mandoc, M. M.; Veurman, W.; Sweelssen, J.; Koetse, M. M.; Blom, P. W. M. *Appl. Phys. Lett.* **2007**, *91*, 073518/1.
(48) McNeil, C. R.; Westenhoff, S.; Friend, R. H.; Greenham, N. C. *J. Phys. Chem. C* **2007**, *111*, 19153.
(49) Quist, P. A. C.; Savenjie, T. J.; Koeste, M. M.; Veenstra, S. C.; Kroon, J. M.; Siebbeles, L. D. A. *Adv. Funct. Mater.* **2005**, *15*, 469.
(50) Mihailetchi, V. D.; Xie, H.; de Boer, B.; Koster, L. J. A.; Blom, P. W. M. *Adv. Funct. Mater.* **2006**, *16*, 699.
(51) Murgatroyd, P. N. *J. Phys. D* **1970**, *3*, 151.
(52) Marsh, R. A.; Groves, C.; Greenham, N. C. *J. Appl. Phys.* **2007**, *101*, 083509/1.

JP901651Z